JOURNAL OF APPLIED ELECTROCHEMISTRY 12 (1982) 469–478

The electrochemistry of partially discharged Planté electrodes

C. LAZARIDES, N. A. HAMPSON

Department of Chemistry, University of Technology, Loughborough, Leicestershire, LE11 3TU, UK

Received 25 November 1981

The electrochemistry of partially discharged Planté electrodes has been investigated. The reduction of partially discharged electrodes continues in the manner expected for a crystallization and growth limited electrode process. The oxidation of partially discharged Planté electrodes is less well defined and it appears that the effects due to nucleation of lead sulphate are removed by the initial discharge from the fully charged condition.

Nomenclature

i	current
Z	number of electrons transferred
F	Faraday
M	molecular weight
ρ	density
h	height of nucleus
t	time
A	rate of nucleation
k	chemical rate constant
N_0	initial number of nuclei
i_m	current maximum
t_m	time at current maximum

1. Introduction

The Planté process is extensively used in England for the production of positive plates for stationary batteries. We have been examining the various stages of the Planté process using pure lead disc electrodes. The effect of perchlorate, the aggressive ion used in the initial part of the formation process, was first examined. Sweeping experiments showed that perchlorate increased the anodic current in the lead/lead sulphate region, by displacing the passivating sulphate ion [1].

Lead dissolves freely in sulphuric acid, in the small potential region near −950 mV against Hg_2SO_4/Hg*. We have shown by rotating disc experiments that additions of even large amounts of perchlorate does not alter the kinetics of the reaction process [2, 3].

The major influence of the perchlorate ion was found during the oxidation of lead sulphate to lead dioxide in dilute sulphuric acid. Our potential step experiments showed that the phase formation process changes from two-dimensional instantaneous nucleation in pure sulphuric acid to two-dimensional progressive when small amounts of perchlorate were added. Increasing the perchlorate ion concentration further altered the nucleation process to three-dimensional growth [4, 5].

Having investigated the effect of the perchlorate, our intention was to examine the behaviour of fully formed Planté electrodes under potential step conditions. This paper contains the results of our experiments, in the positive and negative regions of the open circuit voltage, with fully and partially charged Planté electrodes.

2. Experimental procedures

Experiments were carried out on pure lead electrodes (Koch-Light, 99.999%, area 0.071 cm^2) mounted in Teflon. The preparation and shrouding of the electrode has previously been reported [1]. The electrodes were machined to the required diameter and pushed into a tight fitting Teflon receptor. A spring was then soldered onto the back of the electrode and the receptor was then screwed onto a hollow Teflon holder. The complete unit

* All potentials in this paper are referred to this reference electrode system.

0021–891X/82/040469–10$03.70/0

was finally secured onto the stainless steel shaft of a rotating disc assembly by means of a screw on the Teflon holder. Electrical contact was made by means of a mercury pool at the top of the shaft, thus allowing the electrode to be rotated.

The electrodes were polished on roughened glass, lubricated with triple-distilled water, prior to immersion in the electrolyte solution for the start of the Planté formation process. The electrodes were cathodically 'cleaned' before the commencement of the three-cycle process (1.38 mA cm^{-2}; 30 min). The first two cycles (20 h rate) were carried out in sulphuric acid/perchlorate electrolyte. The electrodes were oxidized and then reduced galvanostatically (1.725 mA cm^{-2}). After the two cycles the reduced electrodes were washed in triple-distilled water and dried slowly to allow the 'sponge' lead to oxidize.

The second formation (third cycle) was then carried out in sulphuric acid (1.210 s.g.) by successive charge and discharge cycles (30 h charge, 1.85 mA cm^{-2}; 6 h dch*, 0.95 mA cm^{-2}; 7 h charge 1.45 mA cm^{-2}; 9 h dch, 0.95 mA cm^{-2}). The electrode was then fully charged and a 10 h capacity test made (0.79 mA cm^{-2}). Only electrodes that passed this test by exhibiting capacities greater than 10 h were used for further study.

The formed positive Planté microelectrodes were finally fully charged (at the 10 h rate) and then discharged to different levels of charge for the potential step experiments. It should be noted that the formation process was carried out in the upward facing position to prevent gas retention in the porous matrix. Potential step experiments were carried out in a conventional cell with the facility to spin the electrode in order to remove any retained gas [1]. Hg/Hg_2SO_4 was the reference electrode used throughout and a lead rod of large surface area was used as a counter electrode. Analar grade sulphuric acid and perchlorate were used for the solution preparation.

The fully formed Planté electrode was first allowed to settle down to the reversible potential (+ 1078 mV) on open circuit before being stepped from this voltage to either the fully charged state (1378 mV) or to more negative potentials.

The electrodes were fully charged after the end of each experiment and then discharged again to the required level in order to ensure that the correct amount of charge was always present.

All experiments were carried out in sulphuric acid (1.210 s.g.) The instrumentation consisted of a Kemitron potentiostat (LCV-2) and pulse generator (PM3); the output was recorded using an X–Y recorder (Bryans Series 26000) for the slow transients and a Digital Storage Oscilloscope (Gould, Advance OS4000) in order to observe the fast responses.

3. Results and discussion

Figure 1 shows the initial part of the current–time transient obtained by stepping a fully charged Planté electrode from the open circuit voltage (OCV) to a more negative potential. The curve consists of a rising part with a sharp peak due to the double layer charging combined with a transient response of a species which reacts more readily than the bulk material. This is followed by a small shoulder, due possibly to the interaction of the reaction of the above species with the phase formation reaction, for which the main transient

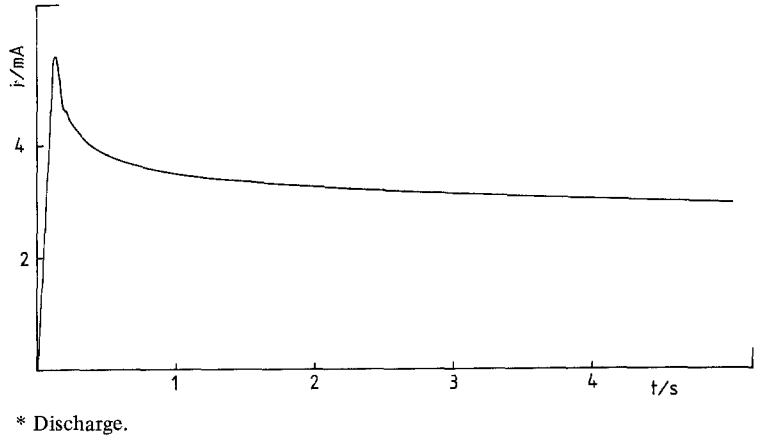

Fig. 1. Current–time transient obtained by stepping the fully charged electrode 75 mV negative of the OCV (1078 mV). Electrolyte; sulphuric acid (1.210 s.g.); 23° C.

* Discharge.

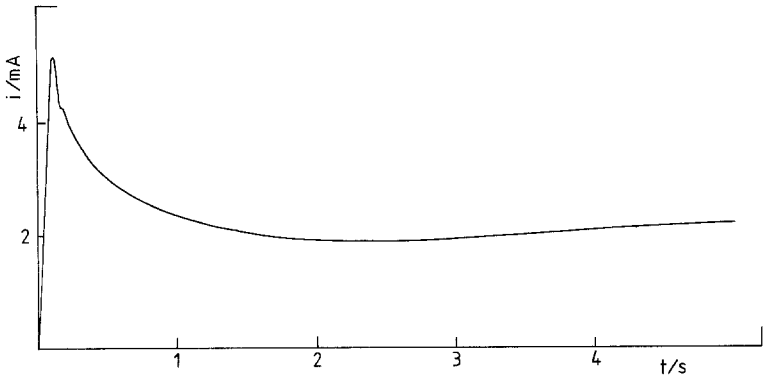

Fig. 2. Current–time transient obtained by stepping the fully charged electrode 90 mV negative of the OCV (1078 mV). Electrolyte; sulphuric acid (1.210 s.g.); 23° C.

represents the current output. The current thereafter falls to zero. Figure 2 shows a similar current–time transient for a pulse 90 mV negative of the OCV. In this case, however, the current starts rising again after the initial fall. A broad peak is eventually formed before the current once more falls to zero. Figure 3 shows the fast part of the current–time transient for a potential step to a potential 160 mV negative of the OCV. In this case the current starts rising immediately after the double layer spike has been formed, producing a peak within three seconds of the start of the experiment. Finally, Figure 4 shows a similar but much sharper response obtained when the electrode was stepped 200 mV negative of the OCV. Figure 5 shows that the current response for the

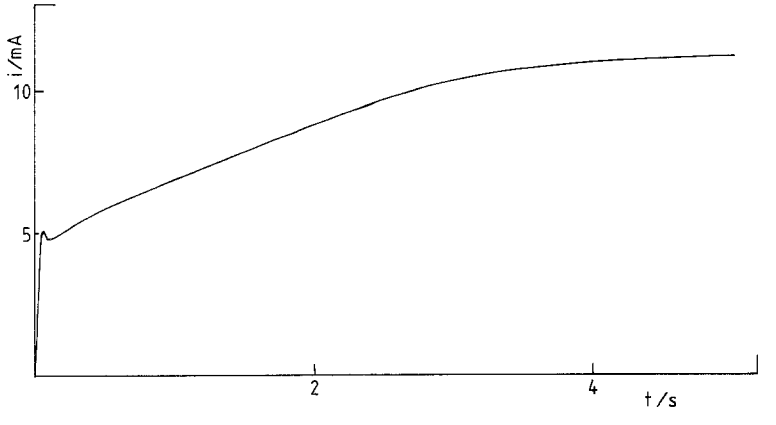

Fig. 3. Current–time transient obtained by stepping the fully charged electrode 160 mV negative of the OCV (1078 mV). Electrolyte; sulphuric acid (1.210 s.g.); 23° C.

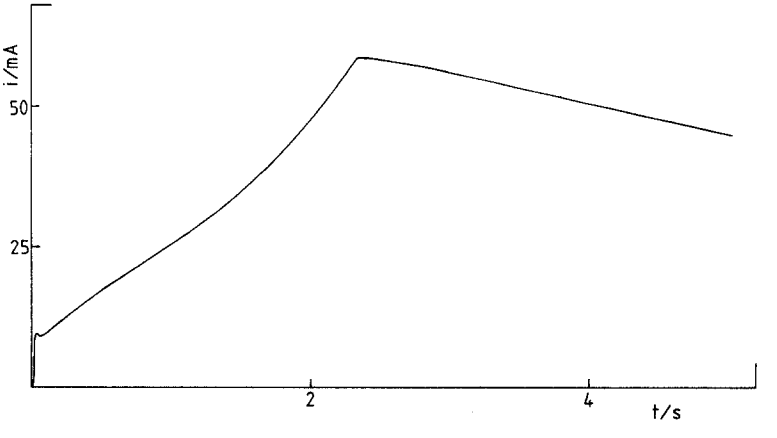

Fig. 4. Current–time transient obtained by stepping the fully charged electrode 200 mV negative of the OCV (1078 mV). Electrolyte; sulphuric acid (1.210 s.g.); 23° C.

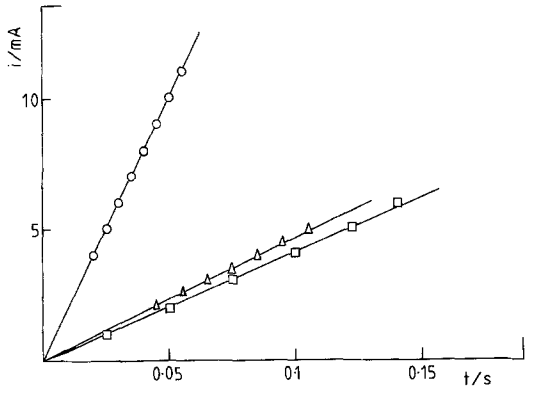

Fig. 5. i versus t for initial rising parts of transients for potential step experiments on fully charged electrodes: △, 1078 to 1003 mV; □, 1078 to 978 mV; ○, 1078 to 951 mV.

rising part of the first peak is proportional to time. Extrapolating to zero time, a zero current intercept was observed for all these responses. This is to be expected as the electrode surface would be uniformely covered with PbO_2, no $PbSO_4$ being present prior to the potential step experiments. The current starts increasing from its zero value as $PbSO_4$ starts forming. Figure 6 shows the complete current–time transient for fully charged Planté microelectrodes at various potentials negative of the OCV. The curves show that the deeper the electrode is stepped into the lead/lead sulphate region the higher the current and the sharper the peaks observed. Analysis of the falling parts of the curves indicated the type of nucleation process taking place.

Figures 7 and 8 show plots of falling parts of the transients for the fully charged electrodes. A $\log_{10}(i/t)$ versus t^2 plot gave the best straight lines showing that the process is a two-dimensional instantaneous growth of lead sulphate which follows the equation [4]

$$i = (zF\pi M/\rho)\, N_0 k^2 t \exp\left[(-\pi M^2 N_0 k^2 t^2)/\rho^2\right]. \quad (1)$$

Electrodes discharged by small amounts (10%,

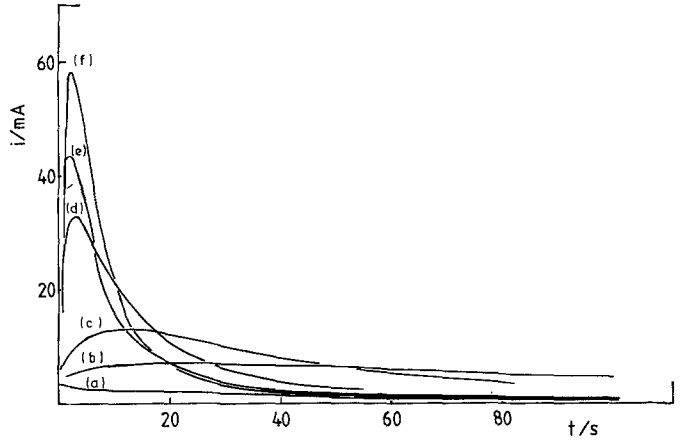

Fig. 6. Series of long time transients for potential step experiments negative of the OCV (fully charged electrodes): (a) 1078 to 1003 mV, (b) 1078 to 978 mV, (c) 1078 to 938 mV, (d) 1078 to 918 mV, (e) 1078 to 898 mV, (f) 1078 to 878 mV. Electrolyte; sulphuric acid (1.210 s.g.); 23° C.

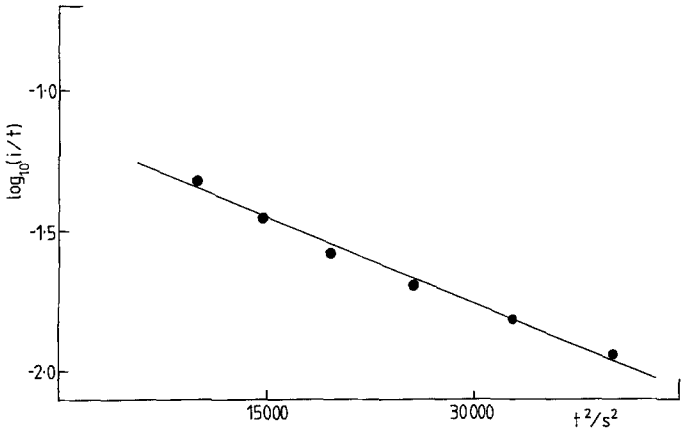

Fig. 7. $\log_{10}(i/t)$ versus t^2 for the falling part of transient (b) in Fig. 6.

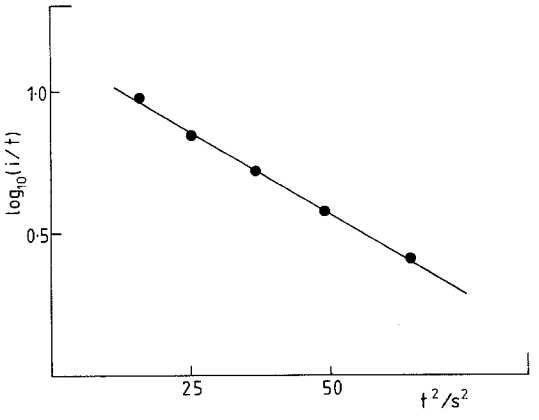

Fig. 8. $\log_{10}(i/t)$ versus t^2 for the falling part of transient (f) in Fig. 6.

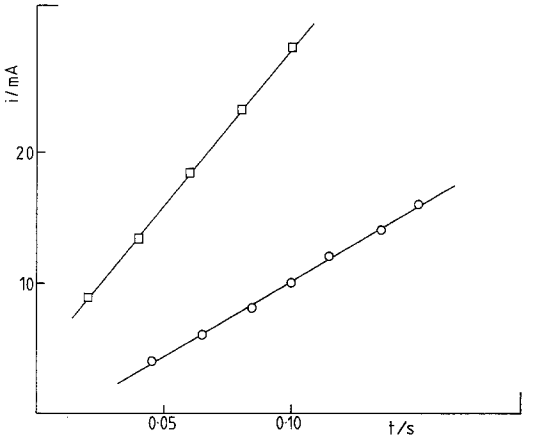

Fig. 9. i versus t for initial rising parts of transients for potential step experiments (1078 to 953 mV) on partially charged electrodes: □, 10% discharge; ○, 20% discharge.

20%) gave similar results to the fully charged electrodes.

Figure 9 shows that the initial rising part of the first peak is still proportional to time. This suggests that the initial growth is again two-dimensional with instantaneous nucleation. The long time parts of the current–time transient are shown in Fig. 10. Analysis of the falling parts of these transients, Fig. 11, indicate that the process is still a two-dimensional instantaneous nucleation. Higher currents are observed again as the electrode is stepped further into the lead sulphate region. These currents are also higher than the equivalent values obtained with the fully charged electrode.

Figure 12 shows that the rising part of the first peak remains proportional to time for various potential step experiments with electrodes discharged to much higher levels. It is interesting to note that only the fully charged electrodes (Fig. 5) show a zero intercept. In theory we would expect the partially discharged electrodes to show a positive intercept due to the fact that there will be some $PbSO_4$ already present. This process is apparently influenced by the fact that the initial discharge was carried out galvanostatically, which would drive the reaction at a fixed rate irrespective of the relative reactivities of the forms of PbO_2 present and independent of the size of the nucleation centres. The responses to a subsequent potentiostatic experiment would be conditioned by the galvanostatic experiments until sufficient new surface ($PbSO_4$) had been formed. The first part of the potentiostatic transient contains a major contribution arising from the galvanostatic conditioning

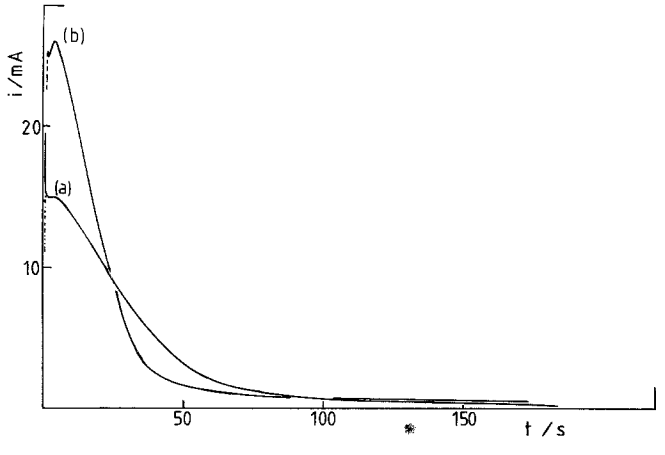

Fig. 10. Current–time transients obtained by stepping 10% discharged electrodes (a) 100 mV and (b) 150 mV negative of the OCV (1078 mV). Electrolyte; sulphuric acid (1.210 s.g.); 23° C.

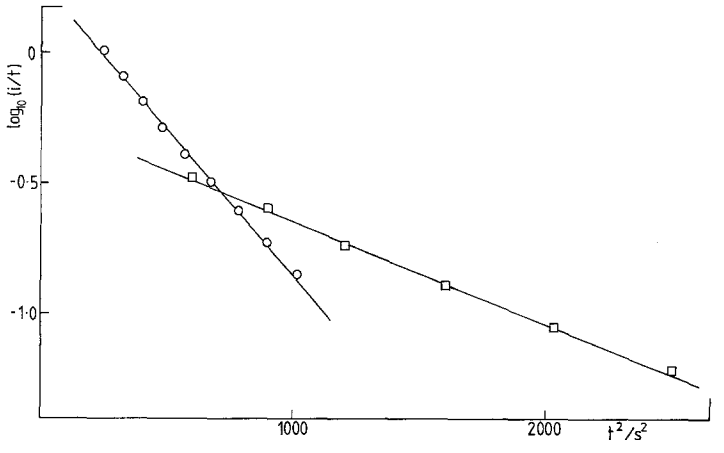

Fig. 11. $\log_{10}(i/t)$ versus t^2 for the falling part of transients in Fig. 10: ○, 1078 to 928 mV; □, 1078 to 978 mV.

of the surface. Later on in the experiment the current rises in the expected manner. The extrapolation to the time axis rather than the current axis reflects this.

Analysis of the falling parts of the transients, proved to be more complicated for the highly discharged electrodes, i.e. those containing a large proportion of $PbSO_4$. Electrodes discharged by 40 and 50% gave straight line plots for both instantaneous and progressive two-dimensional nucleation and growth (Figs. 13a and b), with slightly better correlation coefficients obtained from the progressive nucleation plots, for which the current–time equation [4] is:

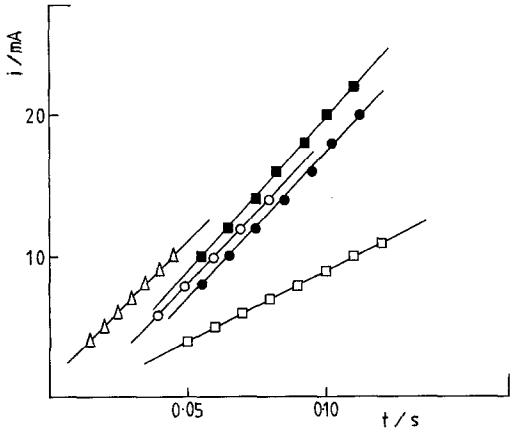

Fig. 12. i versus t for initial rising transients for potential step experiments on partially charged Planté electrodes: ■, 1078 to 953 mV, 40% discharge; ●, 1078 to 928 mV, 40% discharge; □, 1078 to 953 mV, 50% discharge; △, 1078 to 928 mV, 50% discharge; ○, 1078 to 928 mV, 75% discharge.

$$i = (zF\pi M/\rho)\, hA k^2 t^2 \exp\left[(-\pi M^2 A k^2 t^3)/3\rho^2\right]. \quad (2)$$

For the 75% discharged electrode, however, the plots for the falling parts of the transients showed that the process taking place was a three-dimensional progressive nucleation and growth for which the following current–time equation applies [6] for the case of the growth of right circular cones:

$$i = zFk_2\left[1 - \exp\left(-\pi M^2 k_1^2 A t^3/3\rho^2\right)\right] \times \exp\left[(-\pi M^2 k_1^2 A t^3)/3\rho^2\right]. \quad (3)$$

Figures 14a and b show that again there was some indication that the process was a two-dimensional progressive nucleation one, i.e. there was an indication of some two-dimensional progressive character in the three-dimensional process. This could arise if the rate constants for the three-dimensional process were very small in one of the three directions. Table 1 compares instantaneous and progressive nucleation for two-dimensional and three-dimensional processes.

Potential step experiments were also carried out by stepping from the OCV to 1378 mV. This potential was chosen as this was the voltage attained by the fully formed Planté microelectrodes when they were galvanostatically charged to their fully charged state.

Figures 15–18 show the current–time responses for such experiments using fully and partially charged Planté electrodes.

An initial spike is again observed in these experiments which is followed by a second peak

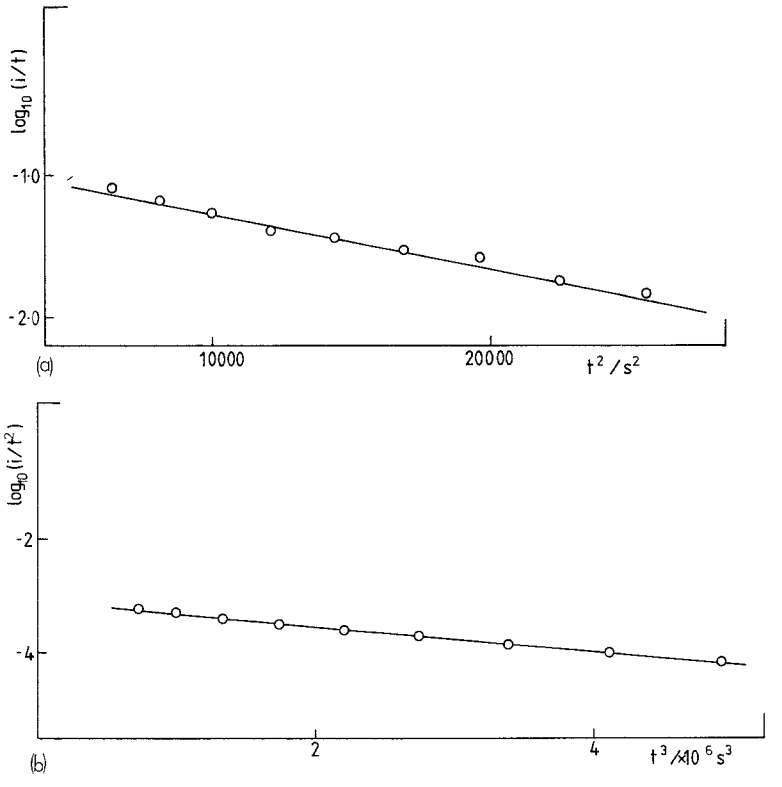

Fig. 13. (a) $\log_{10}(i/t)$ versus t^2 for the falling part of the transient for a 50% discharged electrode. Potential step 1078 to 978 mV. (b) $\log_{10}(i/t^2)$ versus t^3 for the falling part of the transient for a 50% discharged electrode. Potential step 1078 to 978 mV.

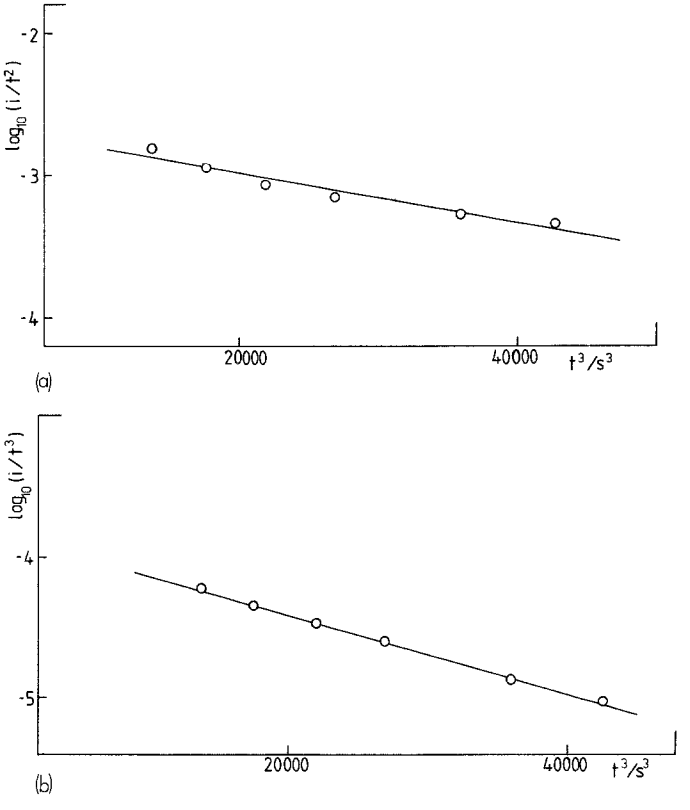

Fig. 14. (a) $\log_{10}(i/t^2)$ versus t^3 for the falling part of the transient for a 75% discharged electrode. Potential step 1078 to 953 mV. (b) $\log_{10}(i/t^3)$ versus t^3 for the falling part of the transient for a 75% discharged electrode. Potential step 1078 to 953 mV.

Table 1. Summary of nucleation and growth processes obtained for potential step experiments from the OCV to potentials in the $PbSO_4$ region. Asterisks (*) indicate the observed model

Percentage discharge	Growth		Nucleation	
	2D	3D	Instantaneous	Progressive
0	*		*	
10	*		*	
20	*		*	
40	*			*
50	*			*
75		*		*

with considerable overlap by the first peak. The current finally decays to zero, indicating completion of the growth of solid-phase PbO_2. It is interesting to note that in addition to these responses, longer time transients for the same experiments show an extra hump for the 40% discharged electrode and two humps for the 75% discharged electrode. These indicate the occurrence of additional electrocrystallization processes in the cases of highly discharged electrodes.

The current magnitudes in these and all other experiments were independent of rotation speed of the electrode. This indicated the lack of any current controlling reaction via the solution.

An exhaustive examination of the falling parts of the transients for the reoxidation of the reduced electrodes was undertaken in order to see if these contained information about the crystallization processes.

The clear picture obtained with the PbO_2 reduction process was not evident in these cases. There was no conformation to the two-dimensional or three-dimensional processes. An attempt to correct the transient data for electrode porosity was made by 'square-rooting' the time dependencies as described by de Levie [7] and also discussed by Lakeman and Hampson [8]. This relatively crude correction produced success in a limited number of cases as typified by the data of

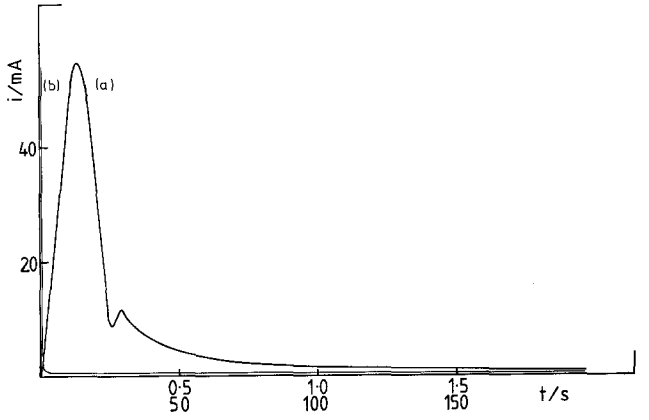

Fig. 15. Current–time transient for fully charged electrode stepped 300 mV positive of OCV (1078 mV). Electrolyte; sulphuric acid (1.210 s.g.); 23° C. (a) Fast response, (b) slow response.

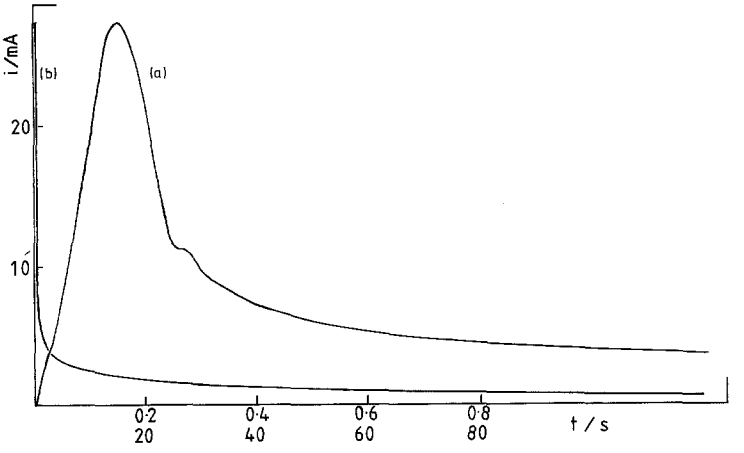

Fig. 16. Current–time transient obtained by stepping a 10% discharged electrode 300 mV positive of OCV. Electrolyte; sulphuric acid (1.210 s.g.); 23° C. (a) Fast response, (b) slow response.

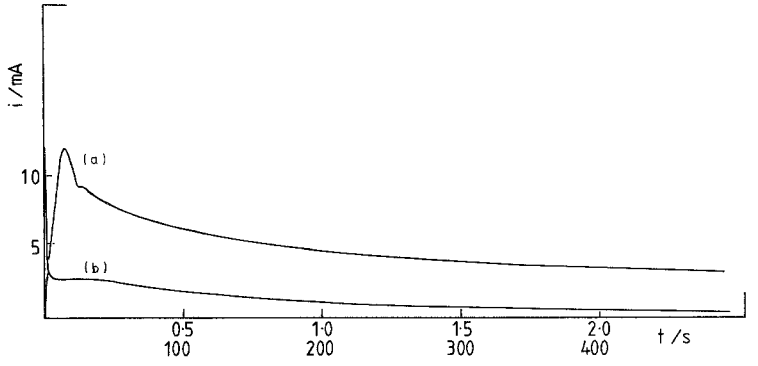

Fig. 17. Current–time transient obtained by stepping a 40% discharged electrode 300 mV positive of OCV. Electrolyte; sulphuric acid (1.210 s.g.); 23° C. (a) Fast response, (b) slow response.

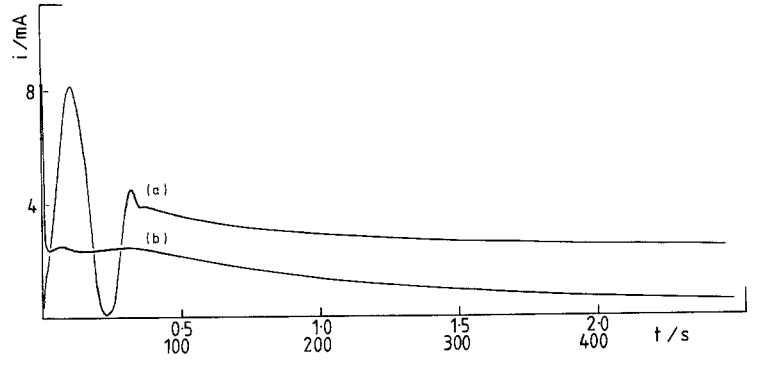

Fig. 18. Current–time transient obtained by stepping a 75% discharged electrode 300 mV positive of OCV. Electrolyte; sulphuric acid (1.210 s.g.); 23° C. (a) Fast response, (b) slow response.

Fig. 19 for 10% discharge which shows that the falling transient at long times could be interpreted as a two-dimensional instantaneous process occurring on the inner surfaces of the porous electrode. Such well defined cases were rare, however, and the data from electrodes discharged to a greater extent yielded no clear picture. The method used by Casson [9] can be used to show the form of the current decay, that is, a simple log i/i_m versus log $(t - t_m)$ presentation. Our data showed two straight line parts, Fig. 20, in a similar manner to the data obtained by Casson [9] but with more negative exponent values indicating a more gradual current decay. Finally, Fig. 21 shows the falling transients presented in terms of log i versus log t for which straight lines were observed.

These results could be explained in terms of a gradual removal of randomly dispersed lead sulphate from a lead dioxide matrix. The number of points on the lead sulphate which can be transformed to lead dioxide is clearly sufficiently large for the nucleation process not to be a current limiting factor since no initial rising transient is observed. The kinetics correspond to the removal

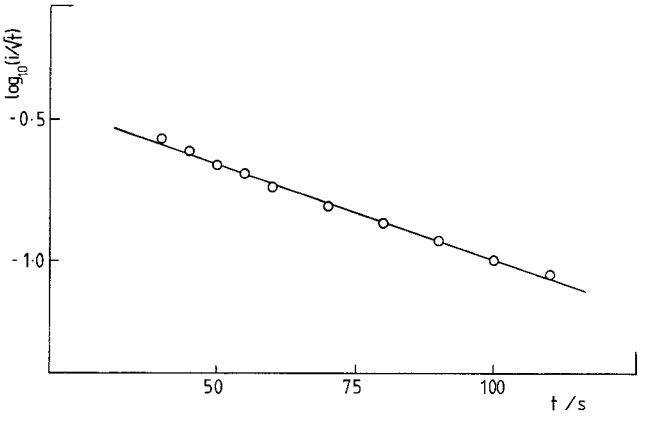

Fig. 19. log $(i/t^{1/2})$ versus t for the falling transient of a 10% discharged electrode, stepped from 1078 to 1378 mV.

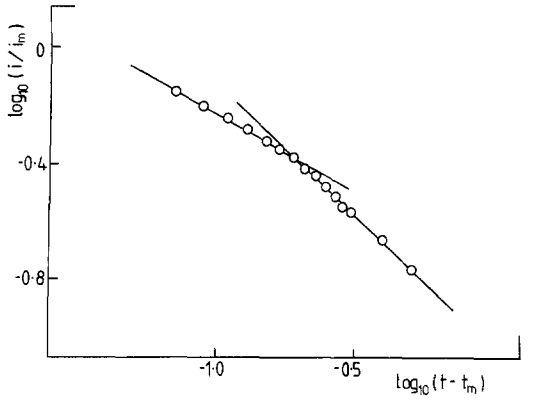

Fig. 20. log (i/i_m) versus log $(t - t_m)$ for the falling transient of a fully charged electrode, stepped from 1078 to 1378 mV.

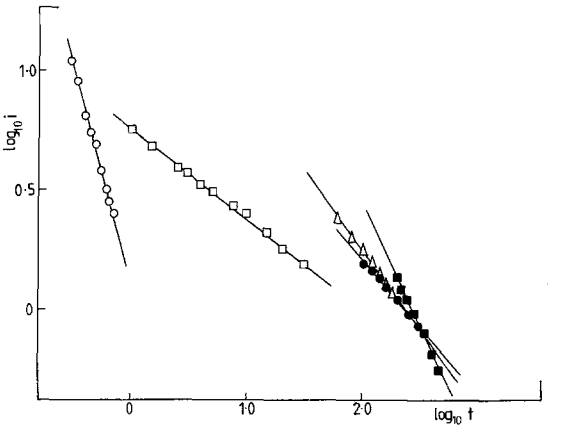

Fig. 21. log i versus log t for the falling transient of potential step experiments from 1078 to 1378 mV, for electrodes in various states of charge: ○, fully charged; □, 10% discharged; △, 40% discharged; ●, 50% discharged; ■, 75% discharged.

of the final traces of lead sulphate particles of varying sizes which have been randomly nucleated by the galvanostatic process. The current might be expected to fall in accordance with the Avrami equation [10–12] which would predict the exponential decay of the type observed.

It does not seem, therefore, that a suitable model exists for the electrocrystallization process for the reoxidation of galvanostatically reduced Planté lead electrodes. This is interesting since the continuation of the reduction process, by a potentiostatic step, behaves in the manner expected. The difference probably lies in the different conductivities of the two phases. In the case of the reduction, an insulating phase is being created whereas in the oxidation a conducting phase is produced. We must conclude that in the presence of significant amounts of lead dioxide, lead sulphate is oxidized, unhampered by nucleation processes, to give a simple falling transient of the form predicted by Canagaratna *et al.* [13].

Acknowledgements

The authors thank the directors of Tungstone Batteries Ltd for financial support (to CL) and permission to publish this paper.

References

[1] C. Lazarides, N. A. Hampson and G. Bulman, *J. Power Sources* **6** (1981) 83.
[2] C. Lazarides, N. A. Hampson, G. Bulman and C. Knowles, Paper No. 40 in 'Power Sources 8', (edited by J. Thompson), Academic Press, London (1981).
[3] N. A. Hampson and C. Lazarides, *Surface Technology* **14** (1981) 301.
[4] C. Lazarides, N. A. Hampson and M. Henderson, *J. Applied Electrochemistry* **11** (1981) 605.
[5] N. A. Hampson, C. Lazarides and M. Henderson, *J. Power Sources* **7** (1981/82) 181.
[6] R. D. Armstrong, M. Fleischmann and H. R. Thirsk, *J. Electroanal. Chem.* **11** (1966) 208.
[7] R. de Levie, in 'Advances in Electrochemical Engineering', Vol. 6 (edited by P. Delahay), Interscience, New York (1967) p. 329.
[8] N. A. Hampson and J. B. Lakeman, *J. Electroanal. Chem.* **107** (1980) 177.
[9] P. Casson, N. A. Hampson and K. Peters, *J. Electroanal. Chem.* **83** (1977) 87.
[10] M. Avrami, *J. Chem. Phys.* **7** (1939) 1103.
[11] M. Avrami, *J. Chem. Phys.* **8** (1940) 212.
[12] M. Avrami, *J. Chem. Phys.* **9** (1941) 177.
[13] S. G. Canagaratna, P. Casson, N. A. Hampson and K. Peters, *J. Electroanal. Chem.* **79** (1977) 273.